# ROLE OF FUNCTIONAL GROUPS ON ADSORPTION AND MICROWAVE REGENERATION OF ACTIVATED CARBON FIBER CLOTH

*Zaher Hashisho, Department of Civil & Environmental Engineering, University of Illinois, Urbana, IL 61801*
*Brenton R. Stone, AFRL/MLQL, 139 Barnes Dr Ste 2, Tyndall AFB, FL 32403*
*Suhail Barot, Department of Electrical & Computer Engineering, University of Illinois, Urbana, IL 61801*
*Mark J. Rood Department of Civil & Environmental Engineering, University of Illinois, Urbana, IL 61801*
*Patrick D. Sullivan, AFRL/MLQL, 139 Barnes Dr Ste 2, Tyndall AFB, FL 32403*
*Jennifer Bernhard, Department of Electrical & Computer Engineering, University of Illinois, Urbana, IL 61801*

## Abstract

Activated Carbon Fiber Cloth (ACFC) is typically regenerated using resistive heating or steam. There is limited information about the regeneration of ACFC using microwave heating, possibly due to the lack of information about its dielectric properties. This research characterizes the impact of functional groups on the adsorption and regeneration properties of virgin, oxidized, and hydrogen ($H_2$)-treated ACFC. Four grades of ACFC were treated with a concentrated acid mixture or with $H_2$ at 950$^o$C. Nitrogen ($N_2$) and water vapor ($H_2O$) adsorption isotherms were obtained to determine the surface areas, distribution of pore sizes and volumes, and adsorption capacities of the virgin and chemically modified ACFCs. X-ray Photoelectron Spectroscopy (XPS) was completed to determine the elemental composition of the samples. The regeneration properties of the resulting ACFC samples were evaluated based on the measurement of their microwave attenuation constants and resistivity. The acid-treated samples contained more oxygen and demonstrated less microwave attenuation and higher resistivity than the virgin samples. In contrast, the $H_2$-treated samples contained less oxygen and demonstrated more microwave attenuation and lower resistivity than the virgin samples. The influence of the chemical treatment on the structure and adsorption of $H_2O$ and $N_2$ is also discussed based on the material characterization tests.

## Introduction

Activated Carbon Fiber Cloth (ACFC) adsorbent is characterized by its high microporosity, adsorption capacity, and purity (Luo *et al.*, 2006). ACFC is typically regenerated using resistive heating or steam. There is limited information about microwave regeneration of ACFC, possibly due to the lack of information about its microwave heating properties. Microwave heating occurs through two primary heating mechanisms: polarization and conduction (Meredith, 1998). Polarization loss is due to coupling of dipolar components of molecules with the alternating electric field which results in frictional losses that manifests itself as heat. Conduction loss is due to electrical resistance within the material that dissipates the energy as heat. In general, conduction losses dominate at low frequencies while polarization heating takes over at frequencies above 1 GHz (Metaxas, 1996).

The need to tailor the adsorption and regeneration properties of adsorbents for specific air quality applications has facilitated a wide range of research activities to modify the physical and chemical properties of activated carbon. In this context, the desire to have more selective adsorption properties for ACFC led to changing the amount of surface-functional groups on the ACFC. For instance, treating ACFC with ammonia enhanced its adsorption capacity for acidic gases such as hydrochloric acid vapors (HCl) and sulfur dioxide ($SO_2$) (Mangun, Benak *et al.,* 2001; Mangun, DeBarr *et al.,* 2001). Similarly, adding oxygen functional groups to ACFC enhanced the adsorption capacity of water vapor (Dimotakis *et al.,* 1995a; Dimotakis *et al.,* 1995b), adsorption of basic compounds such as ammonia, and adsorption of polar compounds such as acetone (Mangun *et al.,* 1999). On the other hand, heat treatment in the presence of hydrogen ($H_2$) at high temperature (950$^o$C) was reported to decompose/desorb surface oxygen groups and produce highly stable carbon adsorbents (Menendez *et al.*, 1996; Basova *et al.*, 1999; Li *et al.*, 2002; Dastgheib and Karanfil, 2004).

While research was completed to modify the electrical properties of ACFC as part of the characterization of ACFC after chemical treatment (Barton and Koresh, 1984; Polovina *et al.*, 1997) or for semi-conductor applications where ACFC is used as a dielectric material for capacitors (Nian and Teng, 2002), no work has been done to modify the electric or dielectric properties of ACFC to enhance its regeneration properties for air pollution control applications. The electrical properties of carbon could also be used as indicators for the progress of the adsorption process and for sensor applications (Del Vecchio *et al.*, 2002; Lukaszewicz, 2006).

ACFC absorbs microwaves and hence is heated by the microwaves (Hashisho *et al.*, 2005; Hashisho *et al.*, 2007); however, it is not clear how the functional groups on the surface of the ACFC affect the absorption of microwaves by ACFC. Making the ACFC less microwave absorbing is expected to further increase the selectivity and hence the energy efficiency of microwave regeneration by depositing the microwave energy directly into the ACFC's pores that possibly contain the microwave absorbing adsorbate. Selective heating of adsorbates that are located in the pores of the adsorbent can reduce the energy needed for regeneration. Such heating could also allow for the separation of the adsorbates during desorption according to their dielectric properties. This could simplify post-regeneration processing when treating a mixture of pollutants with distinct polarity or dielectric properties. On the other hand, making the ACFC more microwave absorbing enhances the heating of ACFC by microwaves, hence allowing for faster, and possibly more efficient, regeneration of the adsorbent. This research investigates the impact of chemical treatment on the adsorption and regeneration properties of ACFC using material characterization tools. Virgin, acid-, and $H_2$-treated ACFC samples were studied using X-ray photoelectron spectroscopy (XPS), nitrogen and water adsorption and desorption, microwave attenuation and resistivity measurements.

## Experimental Methods

***Preparation of the samples***

Samples of virgin ACFC with different degrees of activation (ACFC10, ACFC15, ACFC20 to ACFC25) were dried in an oven at 150 $^{o}$C overnight. $N_2$ flowed through the oven to purge any desorbed water vapor or contaminants.

*Acid treatment*

The oxidized samples were obtained by treating virgin ACFC samples (0.025 $m^2$, 4 g to 7 g) having different degrees of activation with 150 ml of 1/1 (V/V) concentrated $HNO_3$ and $H_2SO_4$ solution for five days (Dimotakis *et al.*, 1995a; Dimotakis *et al.*, 1995b). Samples were then washed with distilled water until neutral pH conditions existed for the water. Samples were then removed from the water and then dried in an oven at 150$^{o}$C in the presence of 200 sccm of $N_2$ flow.

*Hydrogen Treatment*

Four virgin ACFC samples (10 g to 15 g) were heated at 950$^{o}$C in $H_2$ (Menendez *et al.*, 1996; Li *et al.*, 2002). Each sample was put in a quartz boat inside a 4.6 cm inner diameter quartz tube fitted inside a temperature controlled tube furnace (Lindberg furnace, Model 54232; temperature controller unit 59344). The samples were heated in $N_2$ for two hours at 200$^{o}$C to remove chemisorb oxygen and then the gas was switched to $H_2$ (Zero gas grade) at 200 sccm. The samples remained at 950$^{o}$C for three hours, then heating was stopped and the samples were left to cool down. The carrier gas was switched to $N_2$ when the temperature decreased below 100$^{o}$C,

Samples were labeled according to the precursor followed by a suffix referring to the type of treatment (e.g. ACFC15V is not treated (virgin) ACFC15, ACFC15O is acid-treated (oxidized) ACFC15, and ACFC15H is $H_2$-treated ACFC15). The samples were weighted and stored in glass jars that were purged with $N_2$.

***Characterization of the Samples***

*X-ray photoelectron spectroscopy (XPS)*

The elemental content (C, O, N, and S) at the surface of the virgin and chemically-treated ACFC samples was determined using XPS (Perkin-Elmer, Physical Electronics Inc, Model PHI 5400). A sample area of 1 $mm^2$ was targeted with Mg K$\alpha$ or Al K$\alpha$ radiation at 300 W and 15 kV under ultrahigh vacuum ($10^{-8}$ Torr to $10^{-9}$ Torr).

*$N_2$ Isotherms, surface area and pore size distribution*

$N_2$ adsorption isotherms were generated by volumetric measurements (Micromeritics, Inc., Model ASAP 2010). Samples were degassed for more than eight hours at 150°C under vacuum until a pressure of 4 µm Hg – 6 µm Hg. Acid-treated samples were degassed for longer periods compared to the virgin or the $H_2$-treated samples to reach this degassing pressure limit. The adsorption isotherms were obtained at a relative pressure of $10^{-6}$ to 0.99. $N_2$ adsorption and desorption occurred at the boiling point of $N_2$ (77 K). The standard Brunauer, Emmett, and Teller (BET) method was used to fit the adsorption data over a relative pressure range of 0.06 to 0.20. Micropore volume and pore size distribution were determined using the 3D Model (Sun *et al.*, 1998). The 3D Model is based on the Dubinin-Radushkevich (DR) equation and is used to model the adsorption of gases on adsorbents with slit shaped pores and pore sizes between 4 Å and 100 Å. The pore size is defined as the distance between the edges of the carbon atoms in opposite pore walls of the adsorbent. The average micropore size was determined based on the pore size distribution for pore sizes ≤ 20 Å, while the total pore volume was determined based on the volume of $N_2$ adsorbed close to saturation (relative pressure ≅ 0.99) and using the bulk liquid density for $N_2$ (0.808 $cm^3/g$).

*$H_2O$ adsorption/desorption isotherms*

$H_2O$ adsorption/desorption isotherms were collected gravimetrically with a Gravimetric Sorption Analyzer (Model GHP-F, VTI Corporation, FL). The system uses a Magnetic Suspension Balance (Rubotherm, Germany). The mass flow controllers in the system are rated for a nominal 1.0 slpm flow. Approximately 40 mg (about 1 cm x 1.5 cm) of ACFC sample was used for the tests. This Analyzer contains algorithms for generating a specified relative humidity (RH) based on the evaporator temperature, the sample temperature, gas flow rates, and a correlation for the vapor pressure of water. The accuracy of the RH generated by the instrument was verified with a Chilled-Mirror Dew-Point Hygrometer (Edgetech Vigilant™) that was connected in series with this Analyzer. The set-point and measured RH values were within an average 1% RH. $N_2$ was used as the carrier gas throughout the experiments. Each sample was dried at 250° C under $N_2$ prior to each isotherm until a static weight was achieved (<0.03% change in 10 minutes) or for a maximum time of one hour. Isotherms were collected at 25°C and at a RH ranging from 0 to 90% with incremental changes of 5% RH.

*Measurement of dielectric properties*

The attenuation constant is a measure of the rate of decay of an electromagnetic wave as it propagates through a medium (Meredith, 1998). The decay is due to absorption of the microwave energy and its conversion into heat within the medium (Metaxas and Meredith, 1983). As such, higher attenuation constants indicate higher absorption of the electromagnetic field and higher heating as the microwave passes through the targeted material. The microwave attenuation constant for ACFC was studied to better understand the impact of functional groups on the microwave heating of ACFC and how to effectively regenerate ACFC with microwaves. The attenuation constants were determined at a frequency of 2,450 MHz under a controlled environment using a microstrip-based method. About five layers (1.5 cm x 4.5 cm area) of ACFC were mounted into a copper sample holder that had a central conductor that connected the two coaxial connectors on the side of the sample holder (**Figure 1**). The coaxial connectors are connected to a network analyzer (Agilent E8363B) which sent a microwave signal on one side of the sample holder and measure the transmitted signal on the other side of the sample. The attenuation constant was then obtained based on the measurements of the sent and received signal. Before mounting, the samples were dried overnight at 150°C in an oven while $N_2$ flowed through the oven to purge any desorbed water vapor or contaminants. The samples were then stored in sealed glass jars purged with $N_2$ until they are analyzed. Each sample was mounted in the sample holder inside a glove box that was continuously purged with dry and filtered compressed air to provide a controlled RH environment for the ACFC sample. The dry and filtered air was also used to purge the glove box while conducting the measurements.

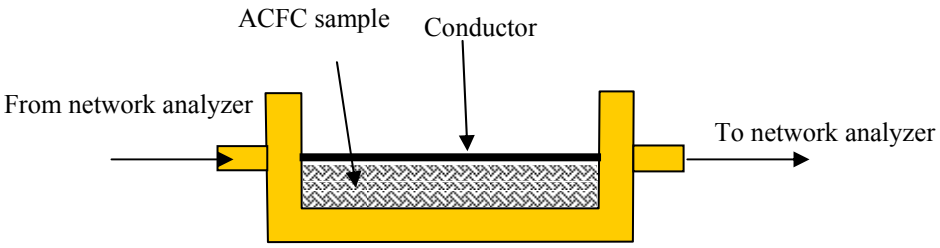


**Figure 1.** Setup for holding the ACFC sample for measurement of the microwave attenuation coefficient

*Resistivity*

The resistivity of ACFC was obtained based on measurements of electrical resistance and dimensions of an ACFC sample at temperatures between 24 $^{o}$C and 210$^{o}$C. A strip of ACFC (width: 1.2 to 4 cm, length: 2 to 6 cm) was attached to two stainless steel electrodes that were connected to a multimeter (Fluke, Model 45) and mounted in a Pyrex chamber which was continuously purged with $N_2$ at 500 sccm. A DC power supply (Tenma, Model 72-2085) connected to the two electrodes or a heating tape wrapped around the Pyrex chamber was used to heat the ACFC sample. The resistance of the ACFC was obtained as the ratio of the measured voltage and current or measured directly with the multimeter. A fluoroptic temperature sensor (Luxtron Inc.) measured the temperature of the ACFC while touching the ACFC sample.

## RESULTS

***XPS of Virgin, and Chemically-Treated ACFC***

Oxidizing the ACFC enriches it with oxygen-containing functional groups such as carboxylic acids, quinones, and phenolic hydroxides. Treating the ACFC samples with the mixture of concentrated $HNO_3$ and $H_2SO_4$ increased the average oxygen content among the samples from 4.5% to 23.9% while the average carbon content decreased from 94.7% to 74.6% (**Table 1**). The average $N_2$ content increased from 0.5% to 1.2% while the average sulfur content increased from 0.21 to 0.25%. The change in the sulfur and nitrogen content of the oxidized samples was small and disproportionate to the increase in the oxygen content, which indicates that the increase in oxygen content is not due to sulfate or nitrate groups from $H_2SO_4$ or $HNO_3$, respectively. On the other hand, heating the ACFC samples at 950$^{o}$C in $H_2$ decreased the average oxygen content among the samples from 4.5% to 1.5%, the average nitrogen content from 0.5% to 0.4% while the average carbon content increased from 94.7% to 98.1%. The change in oxygen content didn't seem to depend on the activation level of the virgin ACFC samples for the acid and $H_2$-treated samples.

**Table 1.** ACFC composition as determined by XPS.

| Sample name | Carbon (%) | Oxygen (%) | Nitrogen (%) | Sulfur (%) |
|---|---|---|---|---|
| ACFC10V | 94.1 | 5.4 | 0.3 | 0.3 |
| ACFC15V | 95.3 | 3.6 | 1.0 | 0.1 |
| ACFC20V | 94.2 | 4.8 | 0.6 | 0.3 |
| ACFC25V | 95.4 | 4.3 | 0.2 | 0.2 |
| ACFC10O | 75.1 | 23.8 | 0.9 | 0.2 |
| ACFC15O | 74.4 | 24.3 | 1.0 | 0.2 |
| ACFC20O | 72.6 | 25.3 | 1.8 | 0.3 |
| ACFC25O | 76.4 | 22.3 | 1.2 | Not available |
| ACFC10H | 98.4 | 1.2 | 0.4 | Not available |
| ACFC15H | 98.7 | 1.1 | 0.2 | Not available |
| ACFC20H | 97.8 | 1.6 | 0.6 | Not available |
| ACFC25H | 97.5 | 2.1 | 0.4 | Not available |

***$N_2$ Adsorption, Surface Area, and Pore Size Distribution of Virgin and Chemically-Treated ACFC***

The $H_2$-treated ACFC depicted comparable BET surface area to virgin ACFC (**Table 2**). The BET surface area increased for both the virgin and the $H_2$-treated ACFC as the degree of activation increased from ACFC10 to ACFC25. On the other hand, BET surface area was comparable for all of the oxidized ACFC, and was lower than that of virgin ACFC. The BET surface area for the oxidized ACFC did not appear to be related to the level of activation of the precursor virgin ACFC.

As is the case for BET surface area, the micropore and total pore volumes for the $H_2$-treated samples were comparable but slightly lower than for the virgin samples. However, the acid-treated samples depicted much lower micropore and total pore volumes compared to the virgin samples. In terms of ratio of micropore to total pore volume, the acid-treated samples depicted a reduction in microporosity for all ACFC activation levels. The $H_2$-treated samples manifested reductions in microporosity, particularly for ACFC10H and ACFC25H.

While the average micropore size was less influenced by the chemical treatment, the average pore size for pores between 4 and 100 Å was much larger for the acid-treated samples. This suggests that acid treatment resulted in

micropores fusing together to form larger pores. On the other hand, both virgin and $H_2$-treated samples depicted similar average micropore and total pore sizes indicating small influence of $H_2$ and heat treatment on the pore structure of ACFC. The decrease in the micropore volume and the absence of prominent effects on the micropore size is consistent with results reported by other researchers (Mangun *et al.*, 1999).

Acid treatment resulted in more changes in the mesopore size distribution when compared to $H_2$ treatment. Acid treatment increased the mean mesopore size. Such change resulted in increasing the average pore size of the acid-treated ACFC. However, $H_2$ treatment doesn't appear to affect the mesopore size distribution. With respect to the micropore size distribution, the impact of acid treatment was most pronounced for ACFC20 and ACFC25 while ACFC10 and ACFC15 depicted smaller change in both micropore and mesopore size distributions. For all ACFC grades, the volume of micropores was much larger than the volume of mesopores reflecting the high microporosity of virgin and chemically-treated ACFC.

**Table 2.** Characterization of ACFC samples using $N_2$ adsorption.

| Sample | BET Surface ($m^2/g$) | Micropore volume ($cm^3/g$) | Total pore volume ($cm^3/g$) | Microporosity (%) | Average micropore size (nm) | Average pore size (nm) |
|---|---|---|---|---|---|---|
| ACFC10-V | 849 | 0.40 | 0.40 | 99.3 | 0.67 | 0.67 |
| ACFC15-V | 1335 | 0.62 | 0.64 | 96.6 | 0.76 | 0.76 |
| ACFC20-V | 1566 | 0.74 | 0.76 | 97.5 | 0.84 | 0.86 |
| ACFC25-V | 1763 | 0.83 | 0.84 | 98.9 | 0.88 | 0.88 |
| ACFC10-O | 793 | 0.33 | 0.38 | 86.1 | 0.70 | 0.73 |
| ACFC15-O | 994 | 0.45 | 0.49 | 91.9 | 0.82 | 0.94 |
| ACFC20-O | 668 | 0.29 | 0.33 | 85.2 | 0.82 | 1.08 |
| ACFC25-O | 873 | 0.37 | 0.44 | 85.0 | 0.85 | 1.11 |
| ACFC10-H | 926 | 0.39 | 0.44 | 88.4 | 0.71 | 0.71 |
| ACFC15-H | 1314 | 0.60 | 0.62 | 95.6 | 0.80 | 0.80 |
| ACFC20-H | 1509 | 0.70 | 0.72 | 97.6 | 0.86 | 0.86 |
| ACFC25-H | 1739 | 0.77 | 0.83 | 93.1 | 0.88 | 0.88 |

To summarize, $H_2$ treatment has a small impact on the samples' micropore and total pore volumes, average micropore size, and BET surface area. However, acid treatment decreases the micropore and total pore volumes, microporosity, and BET surface area. Acid treatment does increase the average pore size and doesn't significantly effect the micropore size distribution. Hence, these results suggest that the addition of oxygenated functional groups by treatment with $HNO_3$ and $H_2SO_4$ mixture resulted in decreasing the volume accessible to $N_2$. It might be that the functional groups have blocked the pores of the ACFC. The large micropores which are readily accessible to nitrates and sulfate ions might be affected more by pore blockage than the small micropores that might be less accessible to those ions. This can justify the reduction in the micropore and total pore volumes. The increase in the mesopore size might be explained by the action of the concentrated acid in etching the carbon structure and/or by fusion of large micropores and small mesopore to form larger pores.

***Adsorption of Water Vapor on Virgin, and Chemically-Treated ACFC***

*Water adsorption isotherms*

Water adsorption on virgin and $H_2$–treated ACFC followed a Type V isotherm according to the Brunauer, Deming, Deming, and Teller (BDDT) classification. This is characterized by low adsorption capacity at low RH values followed by a sharp rise and then a plateau with little increase in adsorption capacity with increasing RH values (**Figure 2**-a and b). During desorption, hysteresis is observed where the desorption branch exists above the adsorption branch indicating that the material can adsorb more water vapor during desorption compared to adsorption. The hysteresis is because the desorption branch represents a thermodynamically more stable phase.

$H_2$ treatment of ACFC didn't have a significant impact on the saturation adsorption capacity since it is controlled by the total pore volume which didn't change significantly after $H_2$ treatment. However, $H_2$ treatment made the step changes in capacity during adsorption and desorption steeper, and shifted the adsorption branch to higher RH values compared to the virgin ACFC reflecting that such treatment made the ACFC more hydrophobic. The shifting of the adsorption to higher RH values and the absence of change in the desorption branch resulted in widening the hysteresis loop for the $H_2$-treated samples compared to the virgin samples. The width of the hysteresis loop increased with increasing level of activation for virgin and $H_2$-treated ACFC samples. Going from ACFC10 to

ACFC25, the activation level and the pore size increased, and the steep rise in the adsorption branch shifted to higher RH values while the location of the steep decrease in the desorption branch appears to be independent of the activation level. This is consistent with the theory of Pierce and Smith (1950), which conceived that the transition from a continuous adsorbed phase to clusters of molecules around the surface oxides occurs at the same relative pressure.

On the other hand, the adsorption of water vapor on the acid-treated ACFC followed a Type I isotherm characterized by an increase in the adsorption capacity with increase in RH followed by leveling of the adsorption isotherm at higher RH values (**Figure 2**-c). Acid treatment had a marked impact on the structure of the water vapor adsorption isotherm as indicated by the increase in adsorption capacity at low RH, the decrease in the saturation adsorption capacity, the disappearance of the sharp changes in adsorption capacity with small changes in RH values for both isotherm branches, the shift in both the adsorption and desorption branches to lower RH values, and the narrowing of the width of the hysteresis loop (**Figure 2**-d). Compared to virgin samples, the acid treated samples depicted higher adsorption capacity at low RH (RH < 40%), indicating an increase in the hydrophilicity of the ACFC, and reflecting its increased polarity. This change in adsorption capacity reflects the impact of oxygen functional groups. However, functional groups are not the only factor affecting the ACFC's adsorption properties. Pore size and volume also affect adsorption as reflected by the reduction in the saturation adsorption capacity due to the smaller pore volume of the acid-treated samples. The shifting of the adsorption branch to low RH values is due to the increase in the affinity of the oxidized ACFC to water vapor because of the enrichment in the oxygenated functional groups which acts as primary adsorption centers (PACs). These PACs will prevent complete desorption until very low RH values which results in narrowing the hysteresis loop (Pierce and Smith, 1950; Dubinin, 1980).

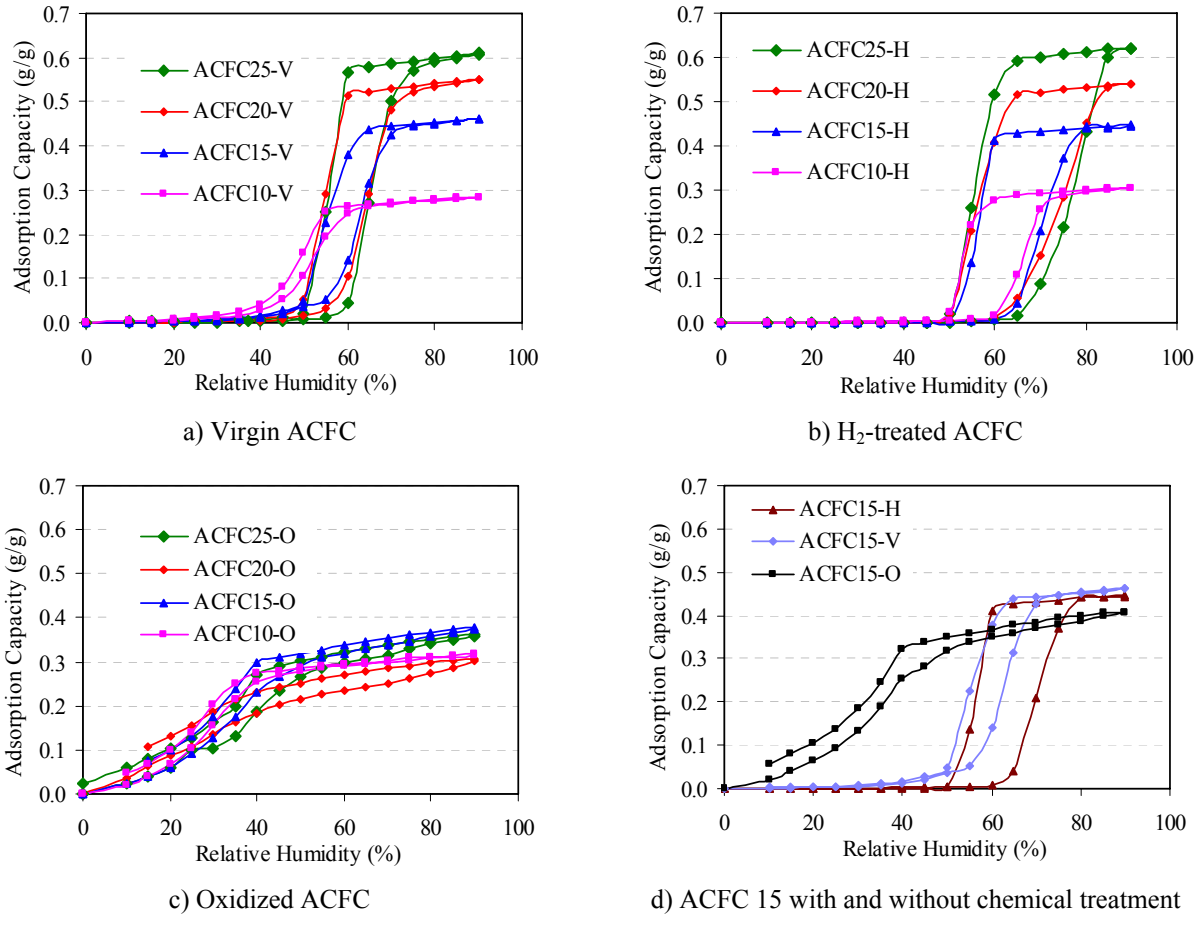


**Figure 2.** Adsorption of water vapor on virgin, oxidized, and $H_2$-treated ACFC

The adsorption of water vapor on the oxidized ACFC reflects the competition between the functional groups and the pore volume available for adsorption. At low RH values, adsorption is controlled by functional groups and the increase in the number of the functional groups result in increased adsorption capacity. However, adsorption is controlled at high RH to near saturation conditions by the pore volume. The decrease in the pore volume for the oxidized ACFC sample results in decreasing the adsorption capacity for water.

Water adsorption and desorption isotherms for virgin, acid-, and $H_2$-treated ACFC15 are compared in **Figure 2**-d. At 65% RH, there is a negligible amount of water adsorbed on the $H_2$-treated samples, while the oxidized and virgin samples have almost achieved their saturation adsorption capacity. Such hydrophobic character of the $H_2$-treated samples is desirable for industrial applications since it reduces the potential for competition between the adsorption of water vapor and other adsorbates (e.g. organic vapors) that need to be removed from gas streams.

*Primary Adsorption Centers*

The water vapor adsorption isotherms were fitted at low to medium RH values (5 to 65%) with the Dubinin-Serpinski (D-Se) isotherm model to determine the number of PACs (Dubinin and Serpinsky, 1981). The PACs are important for the explanation of water adsorption and the formation of hysteresis characterizing water adsorption on porous carbon. The number of PACs, $a_0$, has been used as a measure of the polarity (Bradley, 1997) and hydrohilicity (Kazmierczak *et al.*, 1991) of the surface of activated carbon. The distance between the PACs was related to the mechanism of micropore volume sealing with water molecules (Vartapetyan *et al.*, 1993; Vartapetyan and Voloshchuk, 1995). If the distance between the PACs is greater than the pore width, then sealing of micropores proceeds through the formation of bridge bonds between water molecules adsorbed on the opposite walls of the micropore. If the distance between the PACs is less than the pore width, then the adsorption proceeds with formation of a dense adsorption layer on the micropore's surface.

Water vapor molecules are initially adsorbed in 3-dimensional clusters centered on the PACs (Muller and Gubbins, 1998; Muller *et al.*, 2000; Alcaniz-Monge *et al.*, 2002). These adsorbed water vapor molecules act as secondary adsorption centers which are also capable of forming hydrogen bonds with other water molecules hence where additional water molecules can adsorb. As the relative pressure of water vapor increases, the clusters grow and then merge to form an adsorbed layer that is thermodynamically more stable as it is under the influence of all the active sites (Pierce and Smith, 1950). Hence, during desorption, it is more difficult for the water molecules to desorb, and lower relative pressures are needed for the breakdown of the adsorbed layer into separate clusters.

PACs are associated with oxygen functional groups on carbonaceous adsorbents (Dubinin and Serpinsky, 1981). **Figure 3**-a depicts the variation of $a_0$ with the oxygen content of the ACFC samples. It is interesting that while the oxidized samples have the largest number of PACs, they have the smallest saturation adsorption capacity. This is because the saturation adsorption capacity is determined by the pore volume. However, the oxidized samples have the largest adsorption capacity at low relative pressures where adsorbent-adsorbate interaction becomes more important.

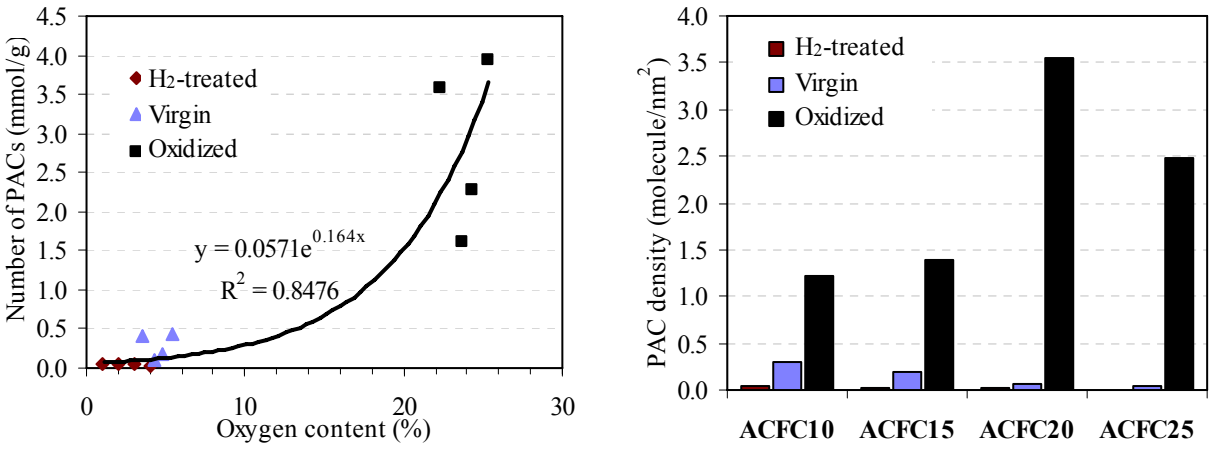


a) PAC vs. oxygen content b) PAC density

**Figure 3.** Variation of the number and density of PACs with oxygen content and type of ACFC treatment

The areal density of PACs was calculated using BET surface area values and the number of PACs based on the D-Se model. Areal density of PACs was highest for the acid-treated samples (**Figure 3**-b). From these densities, the

distance separating the PACs was calculated assuming that the PACs are uniformly distributed on the surface of the ACFC. The distance between PACs for oxidized samples was as low as 0.53 nm which is comparable to the size of a water pentamer cluster (0.5 nm) (Kaneko *et al.*, 1999) and is of the same scale as micropore sizes that range between 0 nm to 2 nm (**Table 2**). $H_2$-treated samples exhibited the largest distance between PACs (10.6 nm). **Figure 4** depicts the variation of the distance between PACs and the relative pressure at the onset of adsorption (relative pressure at the lower step change in the adsorption branch of the isotherm). As the distance between the PACs increases, it becomes more difficult for water vapor to adsorb on the ACFC at low relative pressures. Hence higher relative pressure is needed to have appreciable adsorption of water.

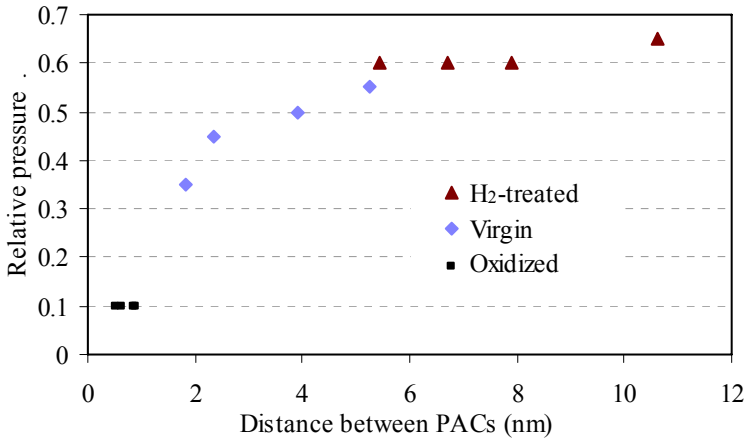


**Figure 4.** Relation between PAC and on set of adsorption

***Dielectric Properties of Virgin, and Chemically-Treated ACFC***

Treating the ACFC with acid deposits oxygenated functional groups on the ACFC. Since oxygen is electronegative, it has high affinity to electrons, and hence it has a tendency to limit the mobility of electrons or negative charge carriers. As such, compared to the virgin samples, the acid-treated samples are expected to exhibit reduced absorption of the microwave energy and reduced attenuation constants due to reduction in their conductivity (**Table 3**). On the other hand, the $H_2$-treated samples have less oxygenated groups, and hence the induced electric current in a microwave field can flow more easily resulting in higher microwave attenuation and heating. This explanation of the impact of functional groups on the attenuation constant of ACFC agrees also the observed change in the resistivity with chemical treatment of ACFC.

**Table 3.** Characterization of microwave attenuation and resistivity of ACFC samples at ambient conditions.

| **Sample** | Resistivity (Ω·m) | Attenuation constant ($cm^{-1}$) |
|---|---|---|
| ACFC10V | 0.0068 | 4.791 |
| ACFC15V | 0.0066 | 3.180 |
| ACFC20V | 0.0127 | 3.352 |
| ACFC25V | 0.0135 | 3.032 |
| ACFC10O | 0.0935 | 1.193 |
| ACFC15O | 0.4208 | 0.220 |
| ACFC20O | 0.3648 | 0.074 |
| ACFC25O | 0.2411 | 0.054 |
| ACFC10H | 0.0027 | 5.724 |
| ACFC15H | 0.0030 | 5.724 |
| ACFC20H | 0.0038 | 5.387 |
| ACFC25H | 0.0051 | 4.709 |

***Resistivity of Virgin, and Chemically-Treated ACFC***

For virgin and $H_2$-treated samples, the resistivity generally increased with increasing level of activation (**Table 3**). This might be due to increased amount of material removed from the sample with increasing levels of activation, which results in increased porosity of the adsorbent and hence decreased cross-section available for current to flow through the adsorbent. For all ACFC activation levels, $H_2$ treatment provided a modest reduction in the resistivity of the virgin ACFC, while acid treatment increased the virgin samples' resistivity by one to two orders of magnitude. The change of resistivity with acid-treatment is consistent with previous reports describing the increase in the DC electric resistance of activated carbon and carbon film after acid treatment or oxygen chemi-adsorption (McLintock and Orr, 1968; Barton and Koresh, 1984; Polovina et al., 1997). Since power dissipation is directly proportional to the resistance and to the square of the electric current, the increase in the resistivity of the acid-treated ACFC sample is manifested in less susceptibility for resistive heating because of the inability of the current to flow through the acid-treated ACFC sample.

## Summary and Conclusion

The wide range in chemical properties among virgin, acid, and $H_2$-treated ACFC samples allowed studying the impact of oxygen functional groups on the adsorption and microwave regeneration properties of ACFC. XPS, $N_2$, and water vapor adsorption and desorption isotherms, and microwave attenuation measurements were used to characterize the virgin and chemically-treated ACFC. The results support the following conclusions:

- Acid treatment increase oxygen content of ACFC while $H_2$ treatment at 950$^o$C reduced the oxygen content of ACFC. In contrast to $H_2$ treatment, acid treatment reduced the saturation adsorption capacity of ACFC to $N_2$ and water vapor.
- Acid treatment reduced the micropore and total volumes, and microporosity of the ACFC; however it didn't have significant impact on the micropore size, and it increased the total pore size. On the other hand, $H_2$ treatment didn't result in significant change in the micropore and total pore volume and size.
- Acid treatment made ACFC more hydrophilic as it increased its adsorption capacity for water vapor at low RH. However it decreased its saturation adsorption capacity. On the other hand, $H_2$ treatment made ACFC more hydrophobic as the step change in the adsorption branch of the isotherm shifted to higher RH values.
- The acid-treated samples demonstrated less microwave attenuation and higher resistivity than the virgin samples. In contrast, the $H_2$-treated samples demonstrated more microwave attenuation and lower resistivity than the virgin samples. These observations are attributed to the electron affinity of the oxygen groups which limits the conduction of current and hence limits the contribution of conductive losses to microwave heating.

## Acknowledgment

The authors acknowledge the financial support from the National Science Foundation (NSF BES 0504385). The XPS and SEM analysis was carried out in the Center for Microanalysis of Materials, University of Illinois at Urbana-Champaign, which is partially supported by the U.S. Department of Energy under grant DEFG02-91ER45439.

## References


Alcaniz-Monge, J., Linares-Solano, A. and Rand, B. 2002. Mechanism of adsorption of water in carbon micropores as revealed by a study of activated carbon fibers. *Journal of Physical Chemistry B*, 106(12): 3209-3216.

Barton, S.S. and Koresh, J.E. 1984. A Study of the Surface Oxides on Carbon Cloth by Electrical-Conductivity. *Carbon*, 22(6): 481-485.

Basova, Y.V., Hatori, H., Yamada, Y. and Miyashita, K. 1999. Effect of oxidation-reduction surface treatment on the electrochemical behavior of PAN-based carbon fibers. *Electrochemistry Communications*, 1(11): 540-544.

Bradley, R.H. 1997. Polar interactions at carbon surfaces described by the Dubinin equations and by an XPS-based model. *Adsorption Science & Technology*, 15(7): 477-484.

Dastgheib, S.A. and Karanfil, T. 2004. Adsorption of oxygen by heat-treated granular and fibrous activated carbons. *Journal of Colloid and Interface Science*, 274(1): 1-8.

Del Vecchio, N.D., Barghi, S. and Puskas, J.E. 2002. New method for monitoring of adsorption column saturation and regeneration I. Demonstration of the measurement principle. *Chemical Engineering Communications*, 189(3): 352-371.

Dimotakis, E., Cal, M., Economy, J., Rood, M. and Larson, S. 1995a. Water vapor adsorption on chemically treated activated carbon cloths. *Chemistry of Materials*, 7(12): 2269-2272.

Dimotakis, E.D., Cal, M.P., Economy, J., Rood, M.J. and Larson, S.M. 1995b. Chemically Treated Activated Carbon Cloths for Removal of Volatile Organic Carbons from Gas Streams - Evidence for Enhanced Physical Adsorption. *Environmental Science & Technology*, 29(7): 1876-1880.

Dubinin, M.M. 1980. Water-Vapor Adsorption and the Microporous Structures of Carbonaceous Adsorbents. *Carbon*, 18(5): 355-364.

Dubinin, M.M. and Serpinsky, V.V. 1981. Isotherm Equation for Water-Vapor Adsorption by Microporous Carbonaceous Adsorbents. *Carbon*, 19(5): 402-403.

Hashisho, Z., Emamipour, H., Cevallos, D., Rood, M., Hay, K.J. and Kim, B.J. 2007. Rapid response concentration-controlled desorption of activated carbon to dampen concentration fluctuations. *Environmental Science and Technology*, 41(5): 1753-1758.

Hashisho, Z., Rood, M. and Botich, L. 2005. Microwave-swing adsorption to capture and recover vapors from air streams with activated carbon fiber cloth. *Environmental Science & Technology*, 39(17): 6851-6859.

Kaneko, K., Hanzawa, Y., Iiyama, T., Kanda, T. and Suzuki, T. 1999. Cluster-mediated water adsorption on carbon nanopores. *Adsorption-Journal of the International Adsorption Society*, 5(1): 7-13.

Kazmierczak, J., Biniak, S., Swiatkowski, A. and Radeke, K.H. 1991. Interdependence of Different Parameters Characterizing the Chemistry of an Activated Carbon Surface. *Journal of the Chemical Society-Faraday Transactions*, 87(21): 3557-3561.

Li, L., Quinlivan, P.A. and Knappe, D.R.U. 2002. Effects of activated carbon surface chemistry and pore structure on the adsorption of organic contaminants from aqueous solution. *Carbon*, 40(12): 2085-2100.

Lukaszewicz, J.P. 2006. Carbon materials for chemical sensors: A review. *Sensor Letters*, 4(2): 53-98.

Luo, L., Ramirez, D., Rood, M.J., Grevillot, G., Hay, K.J. and Thurston, D.L. 2006. Adsorption and electrothermal desorption of organic vapors using activated carbon adsorbents with novel morphologies. *Carbon*, 44(13): 2715-2723.

Mangun, C.L., Benak, K.R., Daley, M.A. and Economy, J. 1999. Oxidation of activated carbon fibers: Effect on pore size, surface chemistry, and adsorption properties. *Chemistry of Materials*, 11(12): 3476-3483.

Mangun, C.L., Benak, K.R., Economy, J. and Foster, K.L. 2001. Surface chemistry, pore sizes and adsorption properties of activated carbon fibers and precursors treated with ammonia. *Carbon*, 39(12): 1809-1820.

Mangun, C.L., DeBarr, J.A. and Economy, J. 2001. Adsorption of sulfur dioxide on ammonia-treated activated carbon fibers. *Carbon*, 39(11): 1689-1696.

McLintock, I.S. and Orr, J.C. 1968. The effect of oxygen adsorption on the electrical resistance of evaporated carbon films. *Carbon*, 6(3): 309-24.

Menendez, J.A., Phillips, J., Xia, B. and Radovic, L.R. 1996. On the modification and characterization of chemical surface properties of activated carbon: In the search of carbons with stable basic properties. *Langmuir*, 12(18): 4404-4410.

Meredith, R.J. 1998. Engineers' handbook of industrial microwave heating. London, Institution of Electrical Engineers.

Metaxas, A.C. 1996. Foundations of electroheat: a unified approach. Chichester; New York, Wiley.

Metaxas, A.C. and Meredith, R.J. 1983. Industrial microwave heating. London, UK, P. Peregrinus on behalf of the Institution of Electrical Engineers.

Muller, E.A. and Gubbins, K.E. 1998. Molecular simulation study of hydrophilic and hydrophobic behavior of activated carbon surfaces. *Carbon*, 36(10): 1433-1438.
Muller, E.A., Hung, F.R. and Gubbins, K.E. 2000. Adsorption of water vapor-methane mixtures on activated carbons. *Langmuir*, 16(12): 5418-5424.
Nian, Y.R. and Teng, H.S. 2002. Nitric acid modification of activated carbon electrodes for improvement of electrochemical capacitance. *Journal of the Electrochemical Society*, 149(8): A1008-A1014.
Pierce, C. and Smith, R.N. 1950. Adsorption-desorption hysteresis in relation to capillarity of adsorbents. *Journal of Physical and Colloidal Chemistry*, 54(6): 784-794.
Polovina, M., Babic, B., Kaluderovic, B. and Dekanski, A. 1997. Surface characterization of oxidized activated carbon cloth. *Carbon*, 35(8): 1047-1052.
Sun, J., Chen, S., Rood, M.J. and Rostam-Abadi, M. 1998. Correlating $N_2$ and $CH_4$ adsorption on microporous carbon using a new analytical model. *Energy & Fuels*, 12(6): 1071-1078.
Vartapetyan, R.S. and Voloshchuk, A.M. 1995. The mechanism of the adsorption of water molecules on carbon adsorbents. *Russian Chemical Reviews*, 64(11): 985.
Vartapetyan, R.S., Voloshchuk, A.M. and Shumilina, E.B. 1993. The Critical Size of Clusters of Water-Molecules on a Carbon Surface. *Russian Chemical Bulletin*, 42(1): 46-48.